

Dielectric properties of $\text{Bi}_{1-x}\text{Sr}_x\text{MnO}_3$ ($x=0.40, 0.50$) manganites: Influence of room temperature charge order

J. L. García-Muñoz,^{1,a)} C. Frontera,¹ B. Rivas-Murias,² and J. Mira²

¹*Institut de Ciència de Materials de Barcelona, CSIC, Campus Universitari de Bellaterra, E-08193 Bellaterra, Spain*

²*Departamento de Física Aplicada, Universidade de Santiago de Compostela, E-15782 Santiago de Compostela, Spain*

(Received 9 December 2008; accepted 5 March 2009; published online 28 April 2009)

The great tendency of Bi–Sr manganites to present charge order (CO) at very high temperatures and partial hybridization of the $6s^2$ lone pair with O p -orbitals makes these materials interesting as potential candidates for obtaining high dielectric constants with very small frequency dependence at room temperature. We have studied the dielectric properties of $\text{Bi}_{1-x}\text{Sr}_x\text{MnO}_3$ ($x=0.40, 0.50$) perovskites that present CO well above room temperature ($T_{\text{CO}} \sim 525$ K). Thick (~ 4 mm) samples exhibit, at room and higher temperatures, high values (above 10^6) of the dielectric constant along a huge range of frequencies in which ϵ_r' is nearly unvarying. The dependence on the thickness of the dielectric constant, its evolution with temperature, and the Cole–Cole diagrams evidence the influence of extrinsic effects. To properly compare the results in the two compounds, we have performed a detailed structural study using neutron and synchrotron diffraction. CO is more extended in $x=0.40$. The results in the two compositions allowed us to correlate CO and phase separation with the huge values of ϵ_r' found in these systems. © 2009 American Institute of Physics. [DOI: 10.1063/1.3116159]

I. INTRODUCTION

High-permittivity dielectric electroceramics attracts considerable attention for applications in the electronics industry. The study of the dielectric properties of different transition metal oxides emerges as a way to find new systems of interest for capacitors, memories, sensors, or actuators. Beside the interest of the magnetoelectric effects, looking for materials with high dielectric constant is a key issue for the development of better capacitive and memory devices.

From a crystallographic point of view, the appearance of a permanent dipolar moment in a material is not compatible with the presence of mirror planes and inversion centers. It has been proposed that charge ordering in oxides can lead to the apparition of colossal dielectric responses.^{1–5} In $\text{Pr}_{2/3}\text{Ca}_{1/3}\text{MnO}_3$, for instance, the high capacitive response disappears just beyond the charge ordering transition temperature.^{1–3} This fact could be linked to the finding that the so called charge order (CO) state drives to the apparition of a noncentrosymmetric structure. For applications, it is important to offer large dielectric responses up to room temperature (RT) and above, in addition to a suitable frequency range. The low transition temperatures in most charge density wave materials represent a strong limitation for their applicability. Concerning CO oxides, the Bi-based manganites clearly deserve specific investigations.

The CO transition in half-doped manganites ($\text{Ln}_{0.5}\text{A}_{0.5}\text{MnO}_3$) presents as common features (i) an increase in the electrical resistivity, (ii) a structural transition to a modulated phase, and at low temperatures, (iii) the development of long-range antiferromagnetic CE-type order. CO is

described as Mn^{3+} and Mn^{4+} separation/ordering in the ionic picture. During the past years Bi–Sr–Mn–O systems has received great attention due to some singularities with respect to the general behavior of the previously studied manganites.^{6–12} One of these is the great tendency of Bi–Sr manganites to present CO at very high temperatures.^{6,9,10,12} Another one is the presence in the electron microscopy images at atomic resolution of internal periodic structures consistent with double stripes of MnO_6 octahedra,^{8,11} which still do not have a convincing justification. The great tendency of Bi–Sr manganites to present CO at very high temperatures [$T_{\text{CO}} \sim 525$ K for $x=0.50$ and $T_{\text{CO}} \sim 625$ K for $x=0.25$ (Ref. 12)] makes these materials interesting as potential candidates for obtaining high dielectric constants with null or very small frequency dependence at RT.

In this paper we studied the dielectric response of two different $\text{Bi}_{1-x}\text{Sr}_x\text{MnO}_3$ compounds ($x=0.40$ and $x=0.50$). Their high T_{CO} is attributed to the particular electronic structure of Bi^{3+} ions ending up, formally, with a $6s^2$ lone pair that has a strong p -character in these compounds. This lone pair hybridizes with O p -orbitals lowering the mobility of Mn e_g electrons and favoring charge localization and ordering. This drives to an unusual behavior in manganites: the charge ordering temperature T_{CO} monotonically increases when decreasing the amount of Sr (increasing the amount of Bi). As a consequence, for the two compositions investigated, it is not necessary to cool down the samples to obtain the charge ordered state, already settled at ambient temperature.

On the other hand, inherent internal inhomogeneities and interfaces can also promote high dielectric values. Phase separation is very usual in these Bi compounds and is

^{a)}Electronic mail: garcia.munoz@icmab.es.

present, systematically, for some ranges of x (for instance, within the interval $0.33 < x < 0.66$). For $x=0.50$ the two coexisting phases present different magnetic ordered structures at low temperature. One of them has mainly the CE magnetic structure usually associated with CO, but the second has an A-type magnetic structure that usually corresponds to charge-delocalized manganites.⁷ The dielectric properties of the $\text{Bi}_{1-x}\text{Sr}_x\text{MnO}_3$ compositions with $x=0.40$ and 0.50 have been investigated in connection with their microscopic nature, as obtained from synchrotron and neutron diffraction data. For the $x=0.50$ sample, the second was extensively reported in Refs. 6 and 7 (based on the same sample used here). For the composition $x=0.40$, a similar diffraction study is presented based on the combination of neutron and synchrotron diffraction techniques. The diffraction and phase separation study shows that, unlike $x=0.50$, in the $x=0.40$ case the two coexisting phases at RT present CO. This is a relevant feature when comparing the dielectric response of $\text{Bi}_{1-x}\text{Sr}_x\text{MnO}_3$ at these two substitution levels ($x=0.40$ and 0.50). Our results help to understand the role of charge ordering for the colossal dielectric phenomenon on manganites.

II. EXPERIMENTAL DETAILS

Polycrystalline samples of $\text{Bi}_{1-x}\text{Sr}_x\text{MnO}_3$ ($x=0.40, 0.50$) were prepared by solid state reaction. High purity SrCO_3 , Bi_2O_3 , and Mn_2O_3 have been mixed at the desired ratios. Initial mixtures have been decarbonated at 900°C for 7 h. After pressing the powders into pellets, the samples have been annealed at 1200°C in air for 15 h. Several regrinding, followed by pressing and annealing have been done. The quality of the samples has been tested by means of laboratory x-ray diffraction. They have been found to be well crystallized and free from impurities up to the detection limit of the technique (~ 1 wt %). Neutron powder diffraction (NPD) data have been collected using D2B ($\lambda=1.542$ Å) diffractometer of the Institute Laue Lagevin in Grenoble, at $T=5$ K and at RT. Ultrahigh resolution synchrotron x-ray powder diffraction (SPD) patterns were collected at ID31 diffractometer of ESRF (Grenoble). The standard Debye–Scherrer configuration was used. Samples were loaded in a borosilicate glass capillary ($\phi=0.3$ mm) and rotated during data collection. A short wavelength, $\lambda=0.429697(6)$ Å, selected with a double-crystal Si (111) monochromator and calibrated with Si NIST ($a=5.43094$ Å), was chosen to reduce the sample absorption and to get the highest intensity. Data were collected at RT, 400, 450, 500, and 600 K.

The complex dielectric permittivity of these samples was measured with a parallel-plate capacitor coupled to a precision LCR meter Agilent 4284A, capable to measure at frequency range from 20 Hz to 1 MHz and from 110 to 350 K. The capacitor was mounted on an aluminum box refrigerated with liquid nitrogen and incorporated a mechanism to control the temperature. The samples were prepared to fit in the capacitor and gold was sputtered on their surfaces to ensure good electrical contact with the electrodes. Additional measurements were performed changing the sample thickness. In

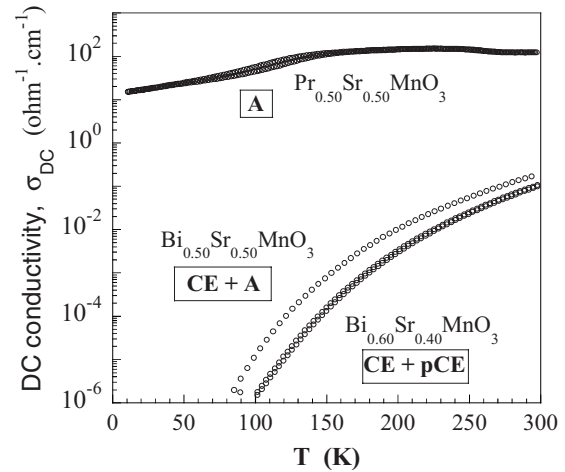


FIG. 1. dc conductivity of $\text{Bi}_{0.6}\text{Sr}_{0.4}\text{MnO}_3$ and $\text{Bi}_{0.5}\text{Sr}_{0.5}\text{MnO}_3$. Temperature dependence and comparison with $\text{Pr}_{0.5}\text{Sr}_{0.5}\text{MnO}_3$. The magnetic order indicated in the figure informs of the presence (CE and pCE) or absence of charge order (A).

addition, to test the optimal performance of the experimental setup, a commercial SrTiO_3 sample was measured and values similar to those reported in literature were obtained.¹³

III. DIELECTRIC RESPONSE CHARACTERIZATION

The conductivity σ_{dc} of the two specimens is depicted in Fig. 1 below RT. It is slightly higher for $x=0.50$ than for $x=0.40$. In the figure it is compared to the half-doped manganite $\text{Pr}_{0.5}\text{Sr}_{0.5}\text{MnO}_3$ (with Pr instead of Bi), which does not exhibit a CO state at any temperature (it presents an A-type magnetic order).

Figures 2(a) and 2(b) show ϵ'_r versus frequency curves

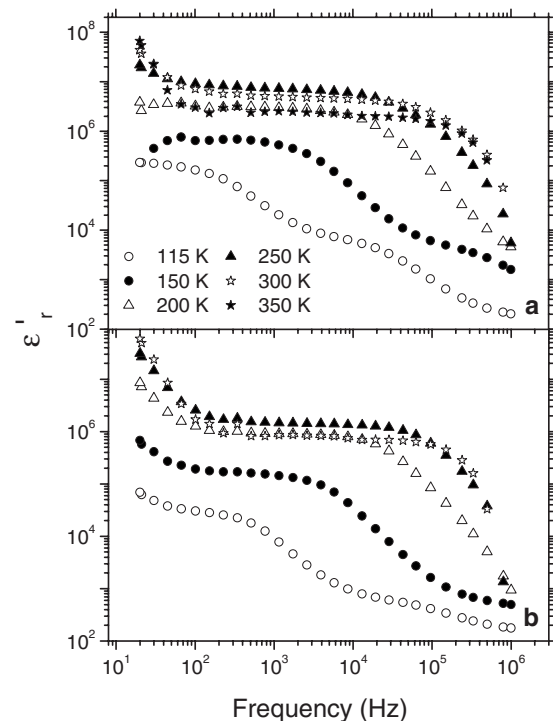


FIG. 2. ϵ'_r vs frequency at selected temperatures corresponding to (a) $\text{Bi}_{0.6}\text{Sr}_{0.4}\text{MnO}_3$ and (b) $\text{Bi}_{0.5}\text{Sr}_{0.5}\text{MnO}_3$ for the thicknesses = 3.8 and 3.9 mm, respectively.

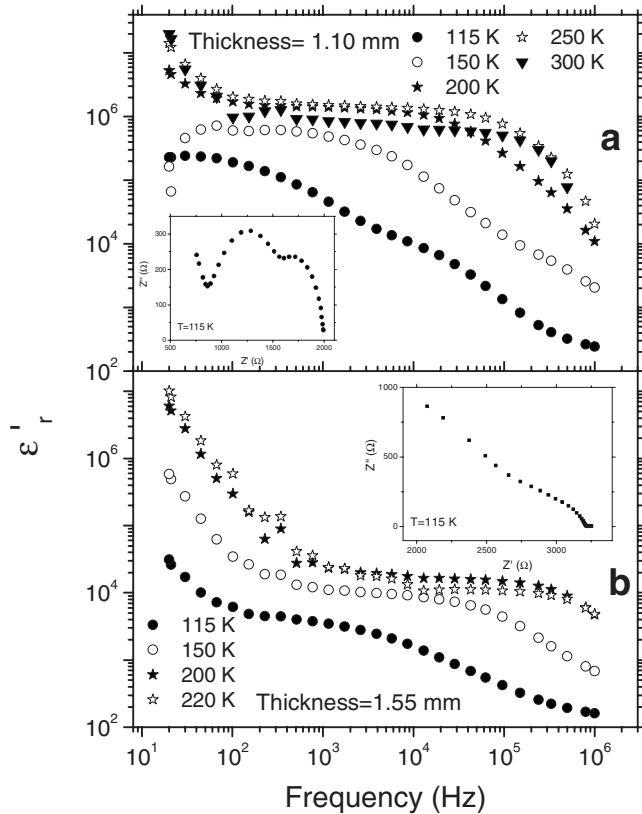


FIG. 3. ϵ'_r vs frequency at selected temperatures corresponding to (a) $\text{Bi}_{0.6}\text{Sr}_{0.4}\text{MnO}_3$, thickness=1.10 mm (top), and (b) $\text{Bi}_{0.5}\text{Sr}_{0.5}\text{MnO}_3$, thickness=1.55 mm (bottom). Insets: Cole–Cole diagram at 115 K.

of $\text{Bi}_{0.6}\text{Sr}_{0.4}\text{MnO}_3$ and $\text{Bi}_{0.5}\text{Sr}_{0.5}\text{MnO}_3$, respectively, for a large distance between the electrodes (sample thickness of ~ 3.8 mm). In both samples, as it can be seen, the dielectric response can be divided into two different behaviors. On one hand, for $T > 150$ K, the dielectric constant keeps high values, above 10^6 , and it is almost constant in a large frequency range. After this, ϵ'_r decreases abruptly at high frequencies. On the other hand, for $T < 150$ K, the dielectric constant shows lower values and a decrease to a constant value in a steplike manner as frequency gets higher.

In order to study the influence of thickness on the dielectric response, we have measured the samples with smaller thicknesses, 1.10 and 1.55 mm for the $\text{Bi}_{0.6}\text{Sr}_{0.4}\text{MnO}_3$ and $\text{Bi}_{0.5}\text{Sr}_{0.5}\text{MnO}_3$ samples, respectively (Fig. 3). We will consider the composition $\text{Bi}_{0.6}\text{Sr}_{0.4}\text{MnO}_3$ first. As it occurs for the case of the thicker $\text{Bi}_{0.6}\text{Sr}_{0.4}\text{MnO}_3$ sample, the dielectric response presents two different behaviors in the studied temperature range [Fig. 3(a)]. From 150 to 300 K, the dielectric constant keeps high values and is almost constant, $\sim 10^6$, in a large frequency range, and afterwards the ϵ'_r value decreases abruptly at high frequencies. The values in Fig. 3(a) are almost an order of magnitude lower than those for the thicker sample. For $T < 150$ K, the dielectric constant shows a decrease in a steplike manner as frequency gets higher. These steps are related to the electrode, grain boundaries, and bulk characteristics. At lower temperatures and higher frequencies, ϵ'_r has a trend toward ~ 200 K. In the inset of Fig. 3(a), we showed the impedance complex plane plot obtained at 115 K. We observed two arcs and the beginning of a third

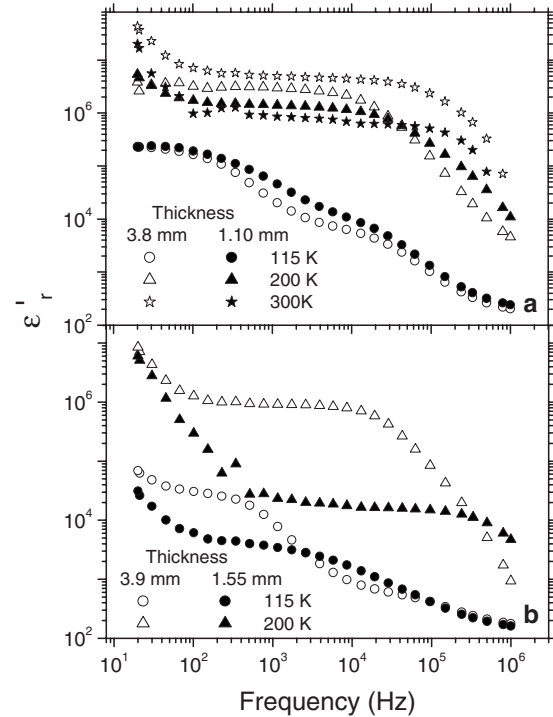


FIG. 4. ϵ'_r vs frequency comparison using two different sample thicknesses for (a) $\text{Bi}_{0.6}\text{Sr}_{0.4}\text{MnO}_3$ and (b) $\text{Bi}_{0.5}\text{Sr}_{0.5}\text{MnO}_3$.

arc but in any case they intercept the origin of coordinates. This fact shows the important role of the extrinsic contributions in the obtained dielectric constant response.

Nevertheless, if we analyse the $\text{Bi}_{0.5}\text{Sr}_{0.5}\text{MnO}_3$ sample with thickness of 1.55 mm, we observe that the frequency dependence of ϵ'_r for this specimen of $\text{Bi}_{0.5}\text{Sr}_{0.5}\text{MnO}_3$ [Fig. 3(b)] presents an initial decrease, followed by a plateau ($\approx 10^2 - 10^5$ Hz). After this plateau, the value decreases and, at lower temperatures and higher frequencies, this value has a trend toward ~ 150 K. In the impedance complex plane plot obtained at 115 K, we observed that it does not intercept the origin of coordinates. As mentioned, this fact corroborates the existence of extrinsic contributions to the dielectric constant values.

In Fig. 4, we show the comparison of ϵ'_r for different sample thicknesses. We observed that for the $\text{Bi}_{0.50}\text{Sr}_{0.50}\text{MnO}_3$ sample [Fig. 4(b)] at higher temperature, the ϵ'_r values change notably. The opposite occurs at lower temperature and higher frequencies, where the values for the different thicknesses are practically the same. This fact is due to the extrinsic contributions to the dielectric constant, being less important in this measured range.

For the $\text{Bi}_{0.60}\text{Sr}_{0.40}\text{MnO}_3$ sample [Fig. 4(a)], we observed that the differences comparing the two thicknesses are notably smaller (relative to differences for the half-doped sample). In addition, apparently the observed differences with thicknesses increase as temperature gets higher.

Finally, when we analyse the frequency dependence of ϵ'_r (without subtracting the dc conductivity) for all the studied samples, we observe that it shows high values that increase almost linearly with temperature. Consequently, the loss tangent ($\tan \delta = \epsilon''_r / \epsilon'_r$) presents high values in the studied temperature range.

IV. THE PRESENCE OF CO INVESTIGATED BY MEANS OF SYNCHROTRON AND NEUTRON DIFFRACTION

The two compositions were characterized by synchrotron and neutron diffraction as a function of temperature between 5 and 650 K. The structural properties of the first specimen ($x=0.50$) were thoroughly described in Refs. 6 and 7. Summarizing, a single-phase diffraction pattern above $T_{CO}=525$ K splits into two phases with very similar lattice parameters below 525 K (see Ref. 6). At low temperature, majority phase (55 wt %) presents a CE-type magnetic order and $\mathbf{q}=1/2\mathbf{a}^*$ structural modulation, indicating orbital and charge ordering below 525 K. Minority phase (45 wt %) adopts at low temperature the A-type magnetic structure and orbital ordering with $\mathbf{q}=0$, implying the absence of CO (Ref. 7) in all the temperature range.

In the present work the same detailed characterization has been extended to the second composition (underdoped sample, $x=0.40$), which has also been studied in the temperature interval of 5–600 K. SPD pattern collected at 600 K (above T_{CO}) can be very well refined ($\chi^2=1.79\%$ and $R_B=3.70\%$) using a single phase with orthorhombic $I bmm$ space group (No. 74). At this temperature, cell parameters obtained [$a=5.509\ 68(2)$ Å, $b=5.495\ 74(2)$ Å, and $c=7.792\ 00(3)$ Å] show a very small distortion with respect to the cubic structure. Patterns collected at the other temperatures (500 K and below) show the coexistence of two different phases and the appearance of small superstructure peaks that can be indexed by doubling a lattice parameter ($\mathbf{q}=1/2\mathbf{a}^*$). NPD and SPD patterns collected at RT can be very well refined (jointly) using two phases with $P bnm$ average cells. Both phases present very similar cell parameters [phase 1 (32 wt %): $a=5.540\ 07(5)$ Å, $b=5.531\ 68(5)$ Å, and $c=7.622\ 02(7)$ Å; phase 2 (68 wt %): $a=5.532\ 33(3)$ Å, $b=5.535\ 29(3)$ Å, and $c=7.653\ 66(5)$ Å] that could be resolved only, thanks to the use of high resolution powder diffractometers [Fig. 5(a)]. In the two samples investigated, the relative fractions of the coexisting phases remain constant below RT.

The low angle region of NPD pattern collected at 5 K shows the presence of several peaks coming from the long-range ordered arrangement of Mn magnetic moments. These peaks can be indexed by doubling both a and b lattice parameters of the coexisting phases and are easily identified from the formation of two different magnetic structures (one corresponding to each phase): the CE magnetic structure for the minority phase and the pseudo-CE magnetic structure^{14,15} for the majority phase. Taking this into consideration, the NPD pattern collected at 5 K can be very well refined [Fig. 5(b)]. For both phases the refined value of the ordered magnetic moment [$\mu_{Mn}=3.7(8)\mu_B$ and $\mu_{Mn}=3.4(4)\mu_B$ for minority and majority phases, respectively] is practically that expected for perfect order ($\mu_{Mn}=3.6\mu_B$). The comparison with the magnetic phases coexisting in $\text{Bi}_{0.50}\text{Sr}_{0.50}\text{MnO}_3$ (Ref. 7) compound is quite revealing. In that case the coexisting magnetic arrangements are the CE and the A type.⁷ To be underlined is that this last structure (A type) is usually not associated with charge ordering in manganites. Thus, our combined SPD and NPD analyses of $x=0.40$ compound demonstrates

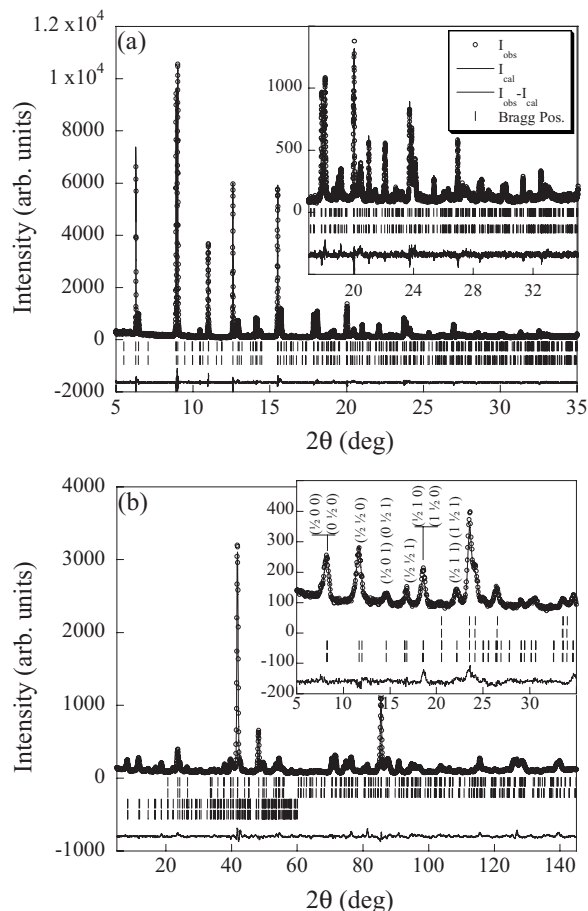


FIG. 5. (a) Rietveld refinement of RT SPD data showing the coexistence of two very similar cells in $\text{Bi}_{0.60}\text{Sr}_{0.40}\text{MnO}_3$. The inset shows in detail the high angular part of the pattern. (b) Rietveld refinement of the low temperature NPD data. The inset shows in detail the low angle part of the pattern with the most intense magnetic diffraction peaks indexed according to structural cells.

that CO extends to the whole compound, while in the $x=0.50$ case, CO only occurs in the majority (55 wt %) phase (but not in the remaining volume, 45 wt %).

V. SUMMARY AND CONCLUSIONS

CO and charge wave materials with very high transition temperatures are interesting potential candidate oxides for obtaining high dielectric constants with very reduced or minimum frequency dependence at RT. Its origin (intrinsic or extrinsic) is a subject of debate.¹⁶ The Bi–Sr manganites present a strong tendency to adopt CO states at very high temperatures, well above RT. So, in this research we have studied the dielectric response of $x=0.40$ and $x=0.50$ members of the family $\text{Bi}_{1-x}\text{Sr}_x\text{MnO}_3$ as a function of the frequency at various temperatures and for two different sample thicknesses.

Samples investigated display different behaviors at different temperatures. For relatively high temperatures (above 150 K and up to our highest temperature, 350 K) the dielectric constant keeps high values, above 10^6 , and a large plateau exists in which ϵ'_r is almost independent of the frequency. At lower temperatures, the dielectric constant present lower values that diminish with the frequency in a

steplike manner. In order to clarify its effect, we have measured samples with two different thicknesses. As a result of the comparison, we found that extrinsic effects are very important in the present study and that they are minimized at low temperature and high frequencies. The value of ϵ_r' obtained at such conditions is higher for $x=0.40$ ($\epsilon_r' \sim 200$) than for $x=0.50$ ($\epsilon_r' \sim 150$), but a further study at higher frequencies would be necessary in order to obtain the intrinsic value.

We have found that both compositions present phase separation in the whole temperature interval of our dielectric study. Our structural and magnetic study reveals similar behavior but also some remarkable differences in the two compounds. Above T_{CO} , the samples are well crystallized in a single phase. The charge ordering transition induces the appearance of two different crystalline phases (phase separation). The respective phase separated fractions are already formed at RT and do not change at decreasing temperature (are the same at 5 K and RT). In the case of $x=0.40$, both phases present the cell distortion and superstructure peak characteristics of charge ordered phases. Consistently, low-temperature NPD data reveal that the coexisting phases in $x=0.40$ present an ordered arrangement of Mn magnetic moments according to the CE and pseudo-CE magnetic structures (respectively, for each phase) with an ordered magnetic moment ($3.6\mu_B/\text{Mn}$) very similar to that expected. The stabilization of these robust magnetic arrangements demonstrates that both coexisting phases present a strong and well defined charge ordering. In contrast, only one of the coexisting phases in $x=0.50$ compound presents charge order (55 wt %, CE-type magnetic structure). The second phase present in the $x=0.50$ compound (45 wt %, A-type magnetic structure) does not present CO. The A-type magnetic structure contains ferromagnetic planes and for the A phase in $x=0.50$ that ferromagnetism is due to charge delocalization within them (absence of CO).

This difference can be related to the higher value of the dielectric constant found in $x=0.40$, the specimen presenting CO in the two coexisting phases in the material ($\approx 100\%$ CO versus $\approx 55\%$ CO in weight for $x=0.50$). In phase separated materials of martensitic nature, like the present ones, domain boundaries and interfaces separating the coexisting phases can act as extrinsic sources for interfacial polarization and Maxwell–Wagner relaxation. The CO/non-CO interfaces

could play a significant role in the dielectric response of these high-temperature CO materials that deserve further studies.

ACKNOWLEDGMENTS

Financial support by the Spanish MICINN (Spanish government) under Project Nos. MAT2006-11080-C02-02 and NANOSELECT CSD2007-00041, and Generalitat de Catalunya (Grant No. 2005-GRQ-00509) is thanked. We thank the European Synchrotron Radiation Facility, Institut Laue-Langevin, and the CRG-D1B for the provision of beam time. The FAME European Network of Excellence is also acknowledged.

- ¹F. Rivadulla, M. A. López-Quintela, L. E. Hueso, C. Jardón, A. Fondado, J. Rivas, M. T. Causa, and R. D. Sánchez, *Solid State Commun.* **110**, 179 (1999).
- ²C. Jardón, F. Rivadulla, L. E. Hueso, A. Fondado, M. A. López-Quintela, J. Rivas, R. Zysler, M. T. Causa, and R. D. Sánchez, *J. Magn. Magn. Mater.* **196**, 475 (1999).
- ³S. Mercone, A. Wahl, A. Pautrat, M. Pollet, and C. Simon, *Phys. Rev. B* **69**, 174433 (2004).
- ⁴J. Mira, A. Castro-Couceiro, M. Sánchez-Andújar, B. Rivas-Murias, J. Rivas, and M. A. Señaris-Rodríguez, *J. Phys. D: Appl. Phys.* **39**, 1192 (2006).
- ⁵A. Nagano, M. Naka, J. Nasu, and S. Ishihara, *Phys. Rev. Lett.* **99**, 217202 (2007).
- ⁶J. L. García-Muñoz, C. Frontera, M. A. García-Aranda, A. Llobet, and C. Ritter, *Phys. Rev. B* **63**, 064415 (2001).
- ⁷C. Frontera, J. L. García-Muñoz, M. A. G. Aranda, A. Llobet, C. Ritter, M. Respaud, and J. Vanacken, *Phys. Rev. B* **64**, 054401 (2001).
- ⁸M. Hervieu, A. Maignan, C. Martin, N. Nguyen, and B. Raveau, *Chem. Mater.* **13**, 1356 (2001).
- ⁹C. Frontera, J. L. García-Muñoz, C. Ritter, L. Mañosa, X. Capdevila, and A. Calleja, *Solid State Commun.* **125**, 277 (2003).
- ¹⁰J. L. García-Muñoz, C. Frontera, M. A. G. Aranda, C. Ritter, A. Llobet, M. Respaud, M. Goiran, H. Rakoto, O. Masson, J. Vanacken, and J. M. Broto, *J. Solid State Chem.* **171**, 84 (2003).
- ¹¹M. Hervieu, S. Malo, O. Perez, P. Beran, C. Martin, and B. Raveau, *Chem. Mater.* **15**, 523 (2003).
- ¹²C. Frontera, J. L. García-Muñoz, M. Hervieu, M. A. G. Aranda, C. Ritter, Ll. Mañosa, X. G. Capdevila, and A. Calleja, *Phys. Rev. B* **68**, 134408 (2003).
- ¹³H. Takashima, R. Wang, N. Kasai, and A. Shoji, *Appl. Phys. Lett.* **83**, 2883 (2003).
- ¹⁴C. Frontera, J. L. García-Muñoz, A. Llobet, C. Ritter, J. A. Alonso, and J. Rodríguez-Cavajal, *Phys. Rev. B* **62**, 3002 (2000).
- ¹⁵J. L. García-Muñoz, C. Frontera, M. Respaud, M. Giot, C. Ritter, and X. G. Capdevila, *Phys. Rev. B* **72**, 054432 (2005).
- ¹⁶N. Biškup, A. de Andrés, J. L. Martínez, and C. Perca, *Phys. Rev. B* **72**, 024115 (2005).